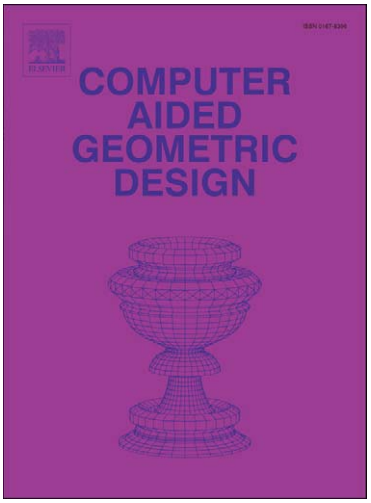

A bound on the approximation of a Catmull-Clark subdivision surface by its limit mesh

Zhangjin Huang, Jiansong Deng, Guoping Wang

PII: S0167-8396(08)00033-2
DOI: 10.1016/j.cagd.2008.05.002
Reference: COMAID 1096

To appear in: *Computer Aided Geometric Design*

Received date: 20 August 2007
Revised date: 29 April 2008
Accepted date: 6 May 2008

Please cite this article as: Z. Huang, J. Deng, G. Wang, A bound on the approximation of a Catmull-Clark subdivision surface by its limit mesh, *Computer Aided Geometric Design* (2008), doi: 10.1016/j.cagd.2008.05.002

A bound on the approximation of a Catmull-Clark subdivision surface by its limit mesh

Zhangjin Huang [a,b,*], Jiansong Deng [c], Guoping Wang [a]

[a] *School of Electronics Engineering and Computer Science, Peking University, Beijing 100871, China*

[b] *Department of Computer Science and Technology, University of Science and Technology of China, Hefei, Anhui 230027, China*

[c] *Department of Mathematics, University of Science and Technology of China, Hefei, Anhui 230026, China*

Abstract

A Catmull-Clark subdivision surface (CCSS) is a smooth surface generated by recursively refining its control meshes, which are often used as linear approximations to the limit surface in geometry processing. For a given control mesh of a CCSS, by pushing the control points to their limit positions, another linear approximation – a *limit mesh* of the CCSS is obtained. In general a limit mesh might approximate a CCSS better than the corresponding control mesh. We derive a bound on the distance between a CCSS patch and its limit face in terms of the maximum norm of the second order differences of the control points and a constant that depends only on the valence of the patch. A subdivision depth estimation formula for the limit mesh approximation is also proposed. For a given error tolerance, fewer subdivision steps are needed if the refined control mesh is replaced with the corresponding limit mesh.

Key words: Catmull-Clark subdivision surfaces, Limit mesh, Distance bound, Subdivision depth

* Corresponding author. Tel.: +86 10 62765819; fax: +86 10 62755798.
Email addresses: zhangjin.huang@gmail.com (Zhangjin Huang), dengjs@ustc.edu.cn (Jiansong Deng), gwang@graphics.pku.edu.cn (Guoping Wang).

1 Introduction

The Catmull-Clark subdivision surface (CCSS) was designed to generalize the bicubic uniform B-spline surface to meshes of arbitrary topology (Catmull and Clark, 1978). Because a CCSS is defined as the limit of a sequence of recursively subdivided control meshes, a linear approximation (for example, a refined control mesh after several steps of subdivision) is often used to approximate the limit surface in applications such as surface rendering, surface trimming, and surface/surface intersection. It is natural to ask the following questions: "How does one estimate the *error (distance)* between a CCSS and its approximation (for instance, the control mesh)?" and "How many (as small as possible) steps of subdivision are needed to satisfy a user-specified error tolerance?". Because of the exponential growth in the number of mesh faces with successive subdivisions, one step, more or one less, can mean a great difference in mesh density. Also, subdivision depth (step) estimation relies on the approximation representation and its error estimate.

Inspired by ideas for computing the bounds on the approximation of polynomials and splines by their control structure (Nairn et al., 1999; Reif, 2000; Lutterkort and Peters, 2001), many efforts have been devoted to estimating error bounds and subdivision depths for subdivision surfaces. Mustafa et al. derived error bounds for general binary and ternary subdivision curves/surfaces in terms of the maximal first order differences of the control points (Mustafa et al., 2006; Mustafa and Deng, 2007). Their bounds work for regular tensor product subdivision surfaces, and, to some extent, have only theoretical values.

As one of the most widely used subdivision surfaces, the CCSS receives more attention than others. The first attempt to derive bounds on the approximation of the CCSS by its control mesh was made by Wang and Qin (2004). Using the distance between the control points and their limits to describe how the control mesh approximates to the limit surface, they derived bounds for the distance between a CCSS and its control mesh and a corresponding subdivision depth estimation method. Their work is based on the assumption that the distance between a CCSS and its control mesh reaches a maximum value at some vertex. But this is not always true. Being aware of this, Cheng and Yong (2006) estimated the distance between a CCSS and its control mesh patch by patch. For a regular patch, the bound is given in terms of the maximum norm of the *second order differences* (called the *second order norm*) of the control points; whereas for an extraordinary patch, the bound is expressed in terms of the *first order norm* of the control points. They also derived a new subdivision depth estimation technique. Then Cheng et al. (2006) improved the error estimate and subdivision depth estimation for an extraordinary CCSS patch by introducing the second order norm into its control mesh. Furthermore, Chen

and Cheng (2006) presented another improvement by using a matrix representation of the second order norm, in the estimate of the convergence rate of the second order norm of an extraordinary CCSS patch. Most recently, Huang and Wang (2007) evaluated the optimal convergence rate of the second order norm by solving constrained minimization problems. Nevertheless, for an extraordinary CCSS patch, the subdivision depth for a given error tolerance is still very large. Since the prior works all focus on the approximation of a CCSS with its control mesh, we turn our attention to other linear approximations.

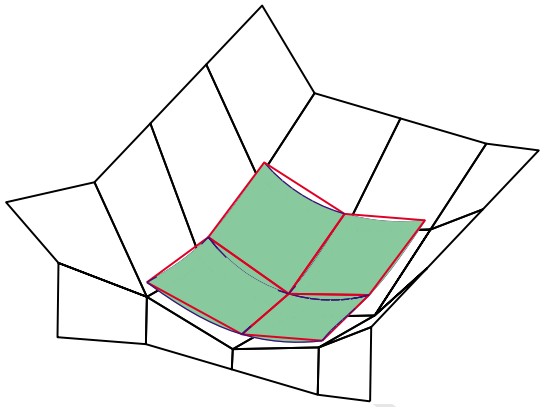

Fig. 1. A Catmull-Clark subdivision surface, its control mesh and the corresponding limit mesh.

Another known linear approximation to a subdivision surface, obtained by pushing the control points of a control mesh to their limit positions, has been applied in surface interpolation (Halstead et al., 1993) and fitting (Hoppe et al., 1994). But the approximation error has not yet been investigated. We reformulate this approximation representation as follows. Extracting a submesh consisting of all interior control points from the control mesh of a CCSS, then pushing the control points to their limit positions, we get a *limit mesh* for the CCSS, which inscribes the limit surface (see Fig. 1). For a closed CCSS, submesh extraction is not needed since its control points are all interior. To bound the distance between a CCSS patch and its limit face, we introduce a distance bound function, and develop a way to find the maximum of the distance bound function for extraordinary cases. The bound reveals that the limit mesh may approximate the limit surface better than the corresponding control mesh in general. Given an error tolerance, the limit mesh approximation needs fewer subdivision steps and fewer mesh faces than the control mesh approximation.

This paper is organized as follows. Section 2 introduces some definitions and notation. In Sections 3 and 4, we derive distance bounds for regular CCSS patches and extraordinary CCSS patches, respectively. And a subdivision depth estimation method for limit mesh approximation is presented in Section 5. In Section 6, we compare limit mesh with control mesh approximation.

Finally we conclude the paper with discussion of future work.

2 Definition and notation

Without loss of generality, we assume the initial control mesh has been subdivided at least twice, isolating the extraordinary vertices so that each face is a quadrilateral and contains at most one extraordinary vertex.

2.1 Distances

Given a control mesh and the corresponding limit mesh of a Catmull-Clark subdivision surface $\tilde{\mathbf{S}}$, for each interior mesh face $\mathbf{F}$ in the control mesh, there is a corresponding *limit face* $\overline{\mathbf{F}}$ in the limit mesh, and a corresponding surface patch $\mathbf{S}$ in the limit surface $\tilde{\mathbf{S}}$. The limit face $\overline{\mathbf{F}}$ is a quadrilateral formed by connecting the four corner points of the patch $\mathbf{S}$.

$2n+8$ control points in the 1-neighborhood of $\mathbf{F}$ form $\mathbf{S}$'s control mesh, where n is the valence of $\mathbf{F}$'s only extraordinary vertex (if it has one and $n = 4$ if not) and called the *valence* of the patch $\mathbf{S}$ (see Fig. 2a). A CCSS patch $\mathbf{S}$ can be parameterized over the unit square $\Omega = [0, 1] \times [0, 1]$ as $\mathbf{S}(u, v)$ (Stam, 1998). Let $\overline{\mathbf{F}}(u, v)$ be the bilinear parameterization of the corresponding limit face $\overline{\mathbf{F}}$ over Ω. For $(u, v) \in \Omega$, we denote $\|\mathbf{S}(u, v) - \overline{\mathbf{F}}(u, v)\|$ as the distance between the points $\mathbf{S}(u, v)$ and $\overline{\mathbf{F}}(u, v)$. The *distance* between a CCSS patch $\mathbf{S}$ and the corresponding limit face $\overline{\mathbf{F}}$ is defined as the maximum distance between $\mathbf{S}(u, v)$ and $\overline{\mathbf{F}}(u, v)$, that is,

$$\max_{(u,v)\in\Omega} \|\mathbf{S}(u, v) - \overline{\mathbf{F}}(u, v)\| \ ,$$

which is also called the distance between the patch $\mathbf{S}$ and the limit mesh of the surface $\tilde{\mathbf{S}}$.

2.2 Second order norms

Let $\Pi = \{\mathbf{P}_i : i = 1, 2, \ldots, 2n + 8\}$ be the control mesh of an extraordinary patch $\mathbf{S} = \mathbf{S}_0^0$, with $\mathbf{P}_1$ being an extraordinary vertex of valence n. The control points are ordered following Stam's method (Stam, 1998) (Fig. 2a). The *second order norm* of Π (or $\mathbf{S}$), denoted $M = M^0 = M_0^0$, is defined as the maximum norm of the following $2n + 10$ *second order differences* (SODs) $\{\alpha_i : i =$

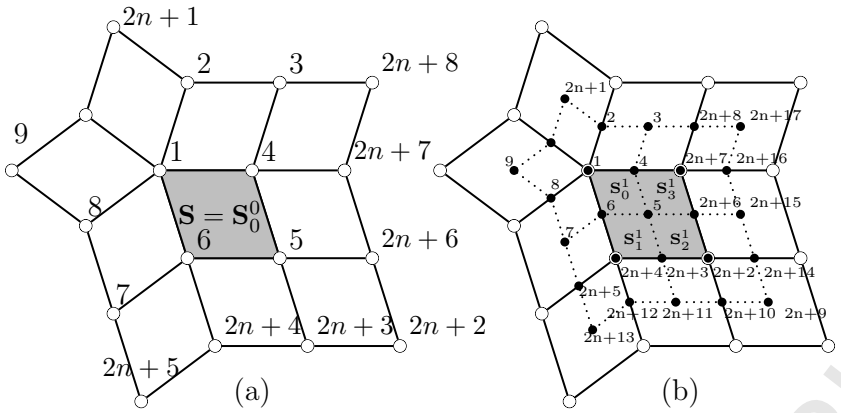

Fig. 2. (a) Ordering of the control points of an extraordinary patch. (b) Ordering of the new control points (solid dots) after a Catmull-Clark subdivision.

$1, \ldots, 2n + 10\}$ of the control points (Cheng et al., 2006):

$$\begin{aligned} M = \max\{&\{\|\mathbf{P}_{2i} - 2\mathbf{P}_1 + \mathbf{P}_{2((i+1)\%n+1)}\| : 1 \le i \le n\} \\ &\cup\{\|\mathbf{P}_{2i+1} - 2\mathbf{P}_{2(i\%n)+2} + \mathbf{P}_{2(i\%n)+3}\| : 1 \le i \le n\} \\ &\cup\{\|\mathbf{P}_2 - 2\mathbf{P}_3 + \mathbf{P}_{2n+8}\|, \|\mathbf{P}_1 - 2\mathbf{P}_4 + \mathbf{P}_{2n+7}\|, \\ &\|\mathbf{P}_6 - 2\mathbf{P}_5 + \mathbf{P}_{2n+6}\|, \|\mathbf{P}_4 - 2\mathbf{P}_5 + \mathbf{P}_{2n+3}\|, \\ &\|\mathbf{P}_1 - 2\mathbf{P}_6 + \mathbf{P}_{2n+4}\|, \|\mathbf{P}_8 - 2\mathbf{P}_7 + \mathbf{P}_{2n+5}\|, \\ &\|\mathbf{P}_{2n+6} - 2\mathbf{P}_{2n+7} + \mathbf{P}_{2n+8}\|, \\ &\|\mathbf{P}_{2n+2} - 2\mathbf{P}_{2n+6} + \mathbf{P}_{2n+7}\|, \\ &\|\mathbf{P}_{2n+2} - 2\mathbf{P}_{2n+3} + \mathbf{P}_{2n+4}\|, \\ &\|\mathbf{P}_{2n+3} - 2\mathbf{P}_{2n+4} + \mathbf{P}_{2n+5}\|\}\} \\ = \max\{&\|\alpha_i\| : i = 1, \ldots, 2n + 10\} \ . \end{aligned} \tag{1}$$

For a regular patch ($n = 4$), there are only two second order differences with the form $\mathbf{P}_{2i} - 2\mathbf{P}_1 + \mathbf{P}_{2((i+1)\%n+1)}$. Thus, the second order norm of a regular patch is defined as the maximum norm of 16 second order differences.

By performing a Catmull-Clark subdivision on Π, one gets $2n+17$ new vertices $\mathbf{P}^1_i, i = 1, \ldots, 2n + 17$ (see Fig. 2b), which are called the *level*-1 *control points* of $\mathbf{S}$. All these level-1 control points compose the *level-1 control mesh* of $\mathbf{S}$: $\Pi^1 = \{P^1_i : i = 1, 2, \ldots, 2n + 17\}$. We use $\mathbf{P}^k_i$ and Π^k to represent the level-k control points and level-k control mesh of $\mathbf{S}$, respectively, after applying k subdivision steps to Π.

The level-1 control points form four control point sets $\Pi^1_0, \Pi^1_1, \Pi^1_2$ and Π^1_3, corresponding to the control meshes of the subpatches $\mathbf{S}^1_0, \mathbf{S}^1_1, \mathbf{S}^1_2$ and $\mathbf{S}^1_3$, respectively (see Fig.2b), where $\Pi^1_0 = \{P^1_i : 1 \le i \le 2n + 8\}$, and the other three control point sets Π^1_1, Π^1_2 and Π^1_3 are shown in Fig. 3. The subpatch $\mathbf{S}^1_0$ is an extraordinary patch, but $\mathbf{S}^1_1, \mathbf{S}^1_2$ and $\mathbf{S}^1_3$ are regular patches. Following the notation in Eq. (1), one can define the second order norms M^1_i for $\mathbf{S}^1_i, i = 0, 1, 2, 3$, respectively. $M^1 = \max\{M^1_i : i = 0, 1, 2, 3\}$ is defined as the

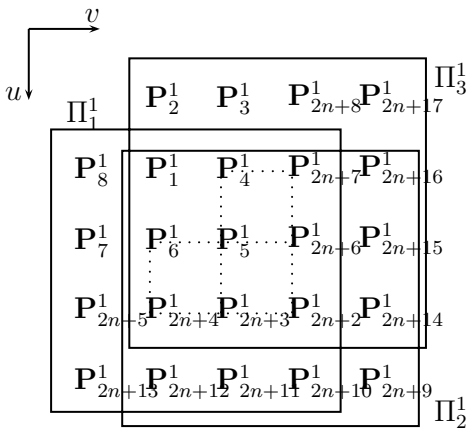

Fig. 3. Control points of the subpatches $\mathbf{S}_1^1, \mathbf{S}_2^1$ and $\mathbf{S}_3^1$.

second order norm of the level-1 control mesh Π^1. After k steps of subdivision on Π, one gets 4^k control point sets $\Pi_i^k : i = 0, 1, \ldots, 4^k - 1$ corresponding to the 4^k subpatches $\mathbf{S}_i^k : i = 0, 1, \ldots, 4^k - 1$ of $\mathbf{S}$, with $\mathbf{S}_0^k$ being the only level-k extraordinary patch (if $n \neq 4$). We denote the second order norms of Π_i^k and Π^k as M_i^k and M^k, respectively.

The second order norms M_0^k and M^0 satisfy the following inequality (Cheng et al., 2006; Chen and Cheng, 2006; Huang and Wang, 2007):

$$M_0^k \leq r_k(n) M^0, \quad k \geq 0 \ , \tag{2}$$

where $r_k(n)$ is called the *k-step convergence rate* of second order norm, which depends on n, the valence of the extraordinary vertex, and $r_0(n) \equiv 1$. Furthermore, it follows that

$$M^k \leq r_k(n) M^0, \quad k \geq 0 \ .$$

An expression for the one-step convergence rate $r_1(n)$ was derived by Cheng et al. (2006) with a direct decomposition method. The multi-step convergence rate $r_k(n)$ was introduced and estimated by Chen and Cheng (2006) with a matrix based technique, then improved by Huang and Wang (2007) with an optimization based approach.

3 Regular patches

In this section, we first express a regular CCSS patch $\mathbf{S}$ and its corresponding limit face $\overline{\mathbf{F}}$ in bicubic Bézier form. Then we bound the distance between $\mathbf{S}$ and $\overline{\mathbf{F}}$ by bounding the distances between their corresponding Bézier points.

If $\mathbf{S}$ is a regular CCSS patch, then $\mathbf{S}(u, v)$ can be expressed as a uniform

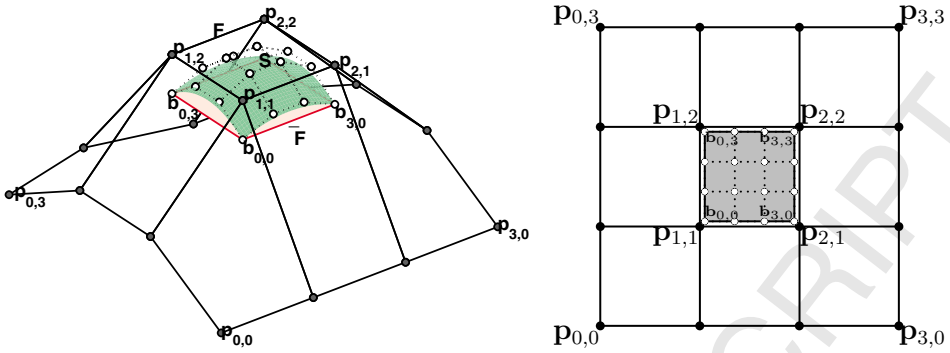

Fig. 4. A regular CCSS patch with its control points (solid dots), the Bézier points (hollow dots) and the limit face.

bicubic B-spline surface patch defined over the unit square Ω with control points $\mathbf{p}_{i,j}, 0 \leq i, j \leq 3$ as follows:

$$\mathbf{S}(u,v) = \sum_{i=0}^{3}\sum_{j=0}^{3} \mathbf{p}_{i,j} N_i^3(u) N_j^3(v) \ , \tag{3}$$

where $N_i^3(u), 0 \leq i \leq 3$ are the uniform cubic B-spline basis functions. $\mathbf{S}(u,v)$ can be converted into the following bicubic Bézier form (Farin, 2002):

$$\mathbf{S}(u,v) = \sum_{i=0}^{3}\sum_{j=0}^{3} \mathbf{b}_{i,j} B_i^3(u) B_j^3(v) \ , \tag{4}$$

where $\mathbf{b}_{i,j}, 0 \leq i, j \leq 3$ are the Bézier points of $\mathbf{S}$ (see Fig. 4), and $B_i^3(u), 0 \leq i \leq 3$ are the cubic Bernstein polynomials. The relationship between $(\mathbf{b}_{i,j})$ and $(\mathbf{p}_{i,j})$ is as follows:

$$\begin{bmatrix} \mathbf{b}_{0,0} & \mathbf{b}_{0,1} & \mathbf{b}_{0,2} & \mathbf{b}_{0,3} \\ \mathbf{b}_{1,0} & \mathbf{b}_{1,1} & \mathbf{b}_{1,2} & \mathbf{b}_{1,3} \\ \mathbf{b}_{2,0} & \mathbf{b}_{2,1} & \mathbf{b}_{2,2} & \mathbf{b}_{2,3} \\ \mathbf{b}_{3,0} & \mathbf{b}_{3,1} & \mathbf{b}_{3,2} & \mathbf{b}_{3,3} \end{bmatrix} = T \begin{bmatrix} \mathbf{p}_{0,0} & \mathbf{p}_{0,1} & \mathbf{p}_{0,2} & \mathbf{p}_{0,3} \\ \mathbf{p}_{1,0} & \mathbf{p}_{1,1} & \mathbf{p}_{1,2} & \mathbf{p}_{1,3} \\ \mathbf{p}_{2,0} & \mathbf{p}_{2,1} & \mathbf{p}_{2,2} & \mathbf{p}_{2,3} \\ \mathbf{p}_{3,0} & \mathbf{p}_{3,1} & \mathbf{p}_{3,2} & \mathbf{p}_{3,3} \end{bmatrix} T^t \ , \tag{5}$$

where

$$T = \frac{1}{6}\begin{bmatrix} 1 & 4 & 1 & 0 \\ 0 & 4 & 2 & 0 \\ 0 & 2 & 4 & 0 \\ 0 & 1 & 4 & 1 \end{bmatrix} \ ,$$

and T^t is the transpose of T.

3.1 Distance bound

Note that the limit points corresponding to $\mathbf{p}_{1,1}$, $\mathbf{p}_{2,1}$, $\mathbf{p}_{2,2}$ and $\mathbf{p}_{1,2}$ are $\mathbf{b}_{0,0}$, $\mathbf{b}_{3,0}$, $\mathbf{b}_{3,3}$ and $\mathbf{b}_{0,3}$, respectively. $\overline{\mathbf{F}} = \{\mathbf{b}_{0,0}, \mathbf{b}_{3,0}, \mathbf{b}_{3,3}, \mathbf{b}_{0,3}\}$ is the limit face corresponding to the center mesh face $\mathbf{F} = \{\mathbf{p}_{1,1}, \mathbf{p}_{2,1}, \mathbf{p}_{2,2}, \mathbf{p}_{1,2}\}$ (see Fig. 4). The bilinear parameterization of $\overline{\mathbf{F}}$ is

$$\overline{\mathbf{F}}(u,v) = (1-v)[(1-u)\mathbf{b}_{0,0} + u\mathbf{b}_{3,0}] + v[(1-u)\mathbf{b}_{0,3} + u\mathbf{b}_{3,3}] \ ,$$

where $(u,v) \in \Omega$. Since $\frac{1}{3}\sum_{i=0}^{3} iB_i^3(t) = t$, we can express $\overline{\mathbf{F}}(u,v)$ as the following bicubic Bézier form:

$$\overline{\mathbf{F}}(u,v) = \sum_{i=0}^{3}\sum_{j=0}^{3} \overline{\mathbf{b}}_{i,j} B_i^3(u) B_j^3(v) \ , \tag{6}$$

where $\overline{\mathbf{b}}_{i,j} = \overline{\mathbf{F}}(\frac{i}{3}, \frac{j}{3}), 0 \le i,j \le 3$ are the Bézier points. It is obvious that $\mathbf{b}_{0,0} = \overline{\mathbf{b}}_{0,0}, \mathbf{b}_{3,0} = \overline{\mathbf{b}}_{3,0}, \mathbf{b}_{0,3} = \overline{\mathbf{b}}_{0,3}, \mathbf{b}_{3,3} = \overline{\mathbf{b}}_{3,3}$.

Hence, for $(u,v) \in \Omega$, it follows that:

$$\begin{aligned} \|\mathbf{S}(u,v) - \overline{\mathbf{F}}(u,v)\| &= \left\| \sum_{i=0}^{3}\sum_{j=0}^{3} (\mathbf{b}_{i,j} - \overline{\mathbf{b}}_{i,j}) B_i^3(u) B_j^3(v) \right\| \\ &\le \sum_{i=0}^{3}\sum_{j=0}^{3} \|\mathbf{b}_{i,j} - \overline{\mathbf{b}}_{i,j}\| B_i^3(u) B_j^3(v) \ . \end{aligned} \tag{7}$$

Let

$$\begin{aligned} M_b = \max\{ &\{\|\mathbf{b}_{i-1,j} - 2\mathbf{b}_{i,j} + \mathbf{b}_{i+1,j}\| : 1 \le i \le 2, 0 \le j \le 3\} \\ &\cup \{\|\mathbf{b}_{i,j-1} - 2\mathbf{b}_{i,j} + \mathbf{b}_{i,j+1}\| : 0 \le i \le 3, 1 \le j \le 2\}\} \end{aligned}$$

be the maximal norm of 16 second order differences of the Bézier points of $\mathbf{S}$. Then we have the following result for the pointwise distance between $\mathbf{S}(u,v)$ and $\overline{\mathbf{F}}(u,v)$:

Lemma 1 *For $(u, v) \in \Omega$, we have*

$$\|\mathbf{S}(u,v) - \overline{\mathbf{F}}(u,v)\| \leq 3(u(1-u) + v(1-v))M_b \ .$$

PROOF. By direct computation, we obtain:

$$\begin{aligned}
\|\mathbf{b}_{1,0} - \overline{\mathbf{b}}_{1,0}\| &= \left\|\frac{2}{3}(\mathbf{b}_{0,0} - 2\mathbf{b}_{1,0} + \mathbf{b}_{2,0}) + \frac{1}{3}(\mathbf{b}_{1,0} - 2\mathbf{b}_{2,0} + \mathbf{b}_{3,0})\right\| \\
&\leq \frac{1}{3}(2\|(\mathbf{b}_{0,0} - 2\mathbf{b}_{1,0} + \mathbf{b}_{2,0})\| + \|(\mathbf{b}_{1,0} - 2\mathbf{b}_{2,0} + \mathbf{b}_{3,0})\|) \\
&\leq M_b \ ,
\end{aligned}$$

and

$$\begin{aligned}
\|\mathbf{b}_{1,1} - \overline{\mathbf{b}}_{1,1}\| = \Big\|&\frac{2}{9}[(\mathbf{b}_{0,0} - 2\mathbf{b}_{1,0} + \mathbf{b}_{2,0}) + (\mathbf{b}_{0,0} - 2\mathbf{b}_{0,1} + \mathbf{b}_{0,2})] \\
&+ \frac{1}{4}[(\mathbf{b}_{0,1} - 2\mathbf{b}_{1,1} + \mathbf{b}_{2,1}) + (\mathbf{b}_{1,0} - 2\mathbf{b}_{1,1} + \mathbf{b}_{1,2})] \\
&+ \frac{1}{6}[(\mathbf{b}_{0,2} - 2\mathbf{b}_{1,2} + \mathbf{b}_{2,2}) + (\mathbf{b}_{2,0} - 2\mathbf{b}_{2,1} + \mathbf{b}_{2,2})] \\
&+ \frac{7}{36}[(\mathbf{b}_{1,0} - 2\mathbf{b}_{2,0} + \mathbf{b}_{3,0}) + (\mathbf{b}_{0,1} - 2\mathbf{b}_{0,2} + \mathbf{b}_{0,3})] \\
&+ \frac{1}{12}[(\mathbf{b}_{1,2} - 2\mathbf{b}_{2,2} + \mathbf{b}_{3,2}) + (\mathbf{b}_{2,1} - 2\mathbf{b}_{2,2} + \mathbf{b}_{2,3})] \\
&+ \frac{1}{36}[(\mathbf{b}_{3,0} - 2\mathbf{b}_{3,1} + \mathbf{b}_{3,2}) + (\mathbf{b}_{0,3} - 2\mathbf{b}_{1,3} + \mathbf{b}_{2,3})] \\
&+ \frac{1}{18}[(\mathbf{b}_{3,1} - 2\mathbf{b}_{3,2} + \mathbf{b}_{3,3}) + (\mathbf{b}_{1,3} - 2\mathbf{b}_{2,3} + \mathbf{b}_{3,3})]\Big\| \\
&\leq 2M_b \ .
\end{aligned}$$

By symmetry, it follows that:

$$\begin{aligned}
&\sum_{i=0}^{3}\sum_{j=0}^{3} \|\mathbf{b}_{i,j} - \overline{\mathbf{b}}_{i,j}\| B_i^3(u) B_j^3(v) \\
&\leq M_b \begin{bmatrix} B_0^3(u) & B_1^3(u) & B_2^3(u) & B_3^3(u) \end{bmatrix} \begin{bmatrix} 0 & 1 & 1 & 0 \\ 1 & 2 & 2 & 1 \\ 1 & 2 & 2 & 1 \\ 0 & 1 & 1 & 0 \end{bmatrix} \begin{bmatrix} B_0^3(v) \\ B_1^3(v) \\ B_2^3(v) \\ B_3^3(v) \end{bmatrix} \\
&= M_b(B_1^3(u) + B_2^3(u) + B_1^3(v) + B_2^3(v)) \\
&= 3(u(1-u) + v(1-v))M_b \ .
\end{aligned}$$

Substituting the above inequality into Eq. (7), we have:

$$\|\mathbf{S}(u,v) - \overline{\mathbf{F}}(u,v)\| \leq 3(u(1-u) + v(1-v))M_b \ .$$

This completes the proof of the lemma. □

Lemma 2 *For a regular CCSS patch* $\mathbf{S}$ *as defined in Eq.* (3)*, the second order norm is*

$$\begin{aligned} M = \max\{&\{\|\mathbf{p}_{i-1,j} - 2\mathbf{p}_{i,j} + \mathbf{p}_{i+1,j}\| : 1 \le i \le 2, 0 \le j \le 3\} \\ &\cup\{\|\mathbf{p}_{i,j-1} - 2\mathbf{p}_{i,j} + \mathbf{p}_{i,j+1}\| : 0 \le i \le 3, 1 \le j \le 2\}\} \ . \end{aligned}$$

It follows that $M_b \le \frac{1}{6}M$*.*

PROOF. By Eq. (5), we have:

$$\begin{aligned} \mathbf{b}_{0,0} =& \frac{1}{36}(\mathbf{p}_{0,0} + 4\mathbf{p}_{1,0} + \mathbf{p}_{2,0}) + \frac{1}{9}(\mathbf{p}_{0,1} + 4\mathbf{p}_{1,1} + \mathbf{p}_{2,1}) \\ &+ \frac{1}{36}(\mathbf{p}_{0,0} + 4\mathbf{p}_{1,0} + \mathbf{p}_{2,0}) \ , \\ \mathbf{b}_{1,0} =& \frac{1}{18}(2\mathbf{p}_{1,0} + \mathbf{p}_{2,0}) + \frac{2}{9}(2\mathbf{p}_{1,1} + \mathbf{p}_{2,1}) + \frac{1}{18}(2\mathbf{p}_{1,2} + \mathbf{p}_{2,2}) \ , \\ \mathbf{b}_{2,0} =& \frac{1}{18}(\mathbf{p}_{1,0} + 2\mathbf{p}_{2,0}) + \frac{2}{9}(\mathbf{p}_{1,1} + 2\mathbf{p}_{2,1}) + \frac{1}{18}(\mathbf{p}_{1,2} + 2\mathbf{p}_{2,2}) \ . \end{aligned}$$

It follows that:

$$\begin{aligned} \|\mathbf{b}_{0,0} - 2\mathbf{b}_{1,0} + \mathbf{b}_{2,0}\| = & \frac{1}{36}\|(\mathbf{p}_{0,0} - 2\mathbf{p}_{1,0} + \mathbf{p}_{2,0}) \\ & +4(\mathbf{p}_{0,0} - 2\mathbf{p}_{1,0} + \mathbf{p}_{2,0}) + (\mathbf{p}_{0,0} - 2\mathbf{p}_{1,0} + \mathbf{p}_{2,0})\| \\ & \le \frac{1}{6}M \ . \end{aligned}$$

Similarly, we have $\|\mathbf{b}_{1,0} - 2\mathbf{b}_{1,1} + \mathbf{b}_{1,2}\| \le \frac{1}{6}M$. By symmetry, the result follows. □

Combining Lemmas 1 and 2, we obtain a bound on the pointwise distance between $\mathbf{S}(u,v)$ and $\overline{\mathbf{F}}(u,v)$:

Theorem 3 *For* $(u,v) \in \Omega$*, we have*

$$\|\mathbf{S}(u,v) - \overline{\mathbf{F}}(u,v)\| \le \frac{1}{2}(u(1-u) + v(1-v))M \ .$$

In the above theorem, $\mathcal{B}(u,v) = \frac{1}{2}(u(1-u) + v(1-v))$ is called the *distance bound function* of $\mathbf{S}(u,v)$ with respect to $\overline{\mathbf{F}}(u,v)$. Since

$$\max_{(u,v)\in\Omega} \mathcal{B}(u,v) = \mathcal{B}(\frac{1}{2},\frac{1}{2}) = \frac{1}{4} \ ,$$

we have a bound on the maximal distance between $\mathbf{S}(u,v)$ and $\overline{\mathbf{F}}(u,v)$ as stated in the following theorem:

Theorem 4 *The distance between a regular CCSS patch* $\mathbf{S}$ *and the corresponding limit face* $\overline{\mathbf{F}}$ *is bounded by*

$$\max_{(u,v)\in\Omega} \|\mathbf{S}(u,v) - \overline{\mathbf{F}}(u,v)\| \leq \frac{1}{4}M \ ,$$

where M *is the second order norm of* $\mathbf{S}$*'s initial control mesh.*

Remark 5 *The distance between a regular patch* $\mathbf{S}$ *and its corresponding center mesh face* $\mathbf{F}$ *is bounded as (Cheng and Yong, 2006):*

$$\max_{(u,v)\in\Omega} \|\mathbf{S}(u,v) - \mathbf{F}(u,v)\| \leq \frac{1}{3}M \ .$$

For regular CCSS patches, these two upper bounds are sharp and achievable. Therefore, Theorem 4 shows that the limit mesh can approximate a uniform bicubic B-spline surface better than the corresponding control mesh in general.

4 Extraordinary patches

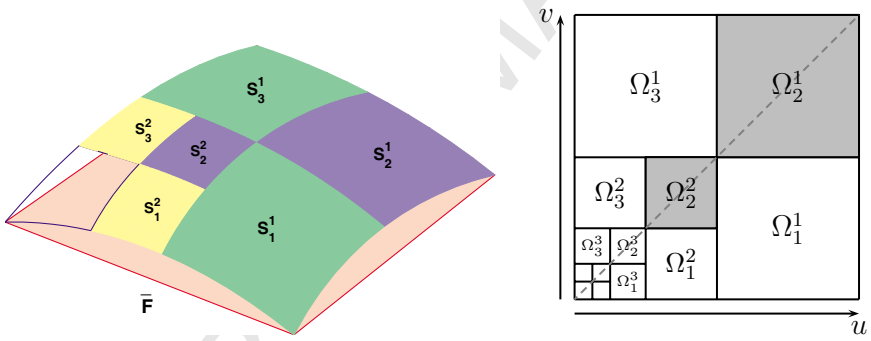

Fig. 5. Partition of an extraordinary CCSS patch (*left*) and Ω-partition of the unit square (*right*).

An extraordinary CCSS patch $\mathbf{S}$ of valence n can be partitioned into an infinite sequence of uniform bicubic B-spline patches $\{\mathbf{S}_m^k\}, k \geq 1, m = 1,2,3$ (see Fig. 5 *left*). If we partition the unit square Ω into an infinite set of tiles $\{\Omega_m^k\}, k \geq 1, m = 1,2,3$, (see Fig. 5 *right*), with

$$\Omega_1^k = \left[\frac{1}{2^k}, \frac{1}{2^{k-1}}\right] \times \left[0, \frac{1}{2^k}\right] \ ,$$
$$\Omega_2^k = \left[\frac{1}{2^k}, \frac{1}{2^{k-1}}\right] \times \left[\frac{1}{2^k}, \frac{1}{2^{k-1}}\right] \ ,$$
$$\Omega_3^k = \left[0, \frac{1}{2^k}\right] \times \left[\frac{1}{2^k}, \frac{1}{2^{k-1}}\right] \ .$$

Each tile Ω_m^k corresponds to a B-spline patch $\mathbf{S}_m^k$, and $\mathbf{S}_m^k(u,v)$ is defined over the unit square with the form as Eq. (3). Therefore, the parameterization for $\mathbf{S}(u,v)$ is constructed as follows (Stam, 1998):

$$\mathbf{S}(u,v) \mid_{\Omega_m^k} = \mathbf{S}_m^k(\tilde{u},\tilde{v}) = \mathbf{S}_m^k(\mathbf{t}_m^k(u,v)) \ ,$$

where the transformation $\mathbf{t}_m^k$ maps the tile Ω_m^k onto the unit square Ω:

$$\begin{aligned}
&\mathbf{t}_1^k(u,v) = (2^k u - 1, 2^k v) \ , \\
&\mathbf{t}_2^k(u,v) = (2^k u - 1, 2^k v - 1) \text{ and} \\
&\mathbf{t}_3^k(u,v) = (2^k u, 2^k v - 1) \ .
\end{aligned}$$

The center face of $\mathbf{S}$'s control mesh is $\mathbf{F} = \{\mathbf{P}_1, \mathbf{P}_6, \mathbf{P}_5, \mathbf{P}_4\}$ (see Fig. 2). The corresponding limit face is $\overline{\mathbf{F}} = \{\overline{\mathbf{P}}_1, \overline{\mathbf{P}}_6, \overline{\mathbf{P}}_5, \overline{\mathbf{P}}_4\}$, with $\overline{\mathbf{P}}_i$ being the limit point of $\mathbf{P}_i, i = 1, 4, 5, 6$. Let $\overline{\mathbf{F}}(u,v)$ be the bilinear parameterization of $\overline{\mathbf{F}}$:

$$\overline{\mathbf{F}}(u,v) = (1-v)[(1-u)\overline{\mathbf{P}}_1 + u\overline{\mathbf{P}}_6] + v[(1-u)\overline{\mathbf{P}}_4 + u\overline{\mathbf{P}}_5] \ , \tag{8}$$

where $(u,v) \in \Omega$. The limit face $\overline{\mathbf{F}}$ can be partitioned into subfaces defined over Ω_m^k as follows:

$$\overline{\mathbf{F}}(u,v) \mid_{\Omega_m^k} = \widehat{\mathbf{F}}_m^k(\mathbf{t}_m^k(u,v))) \ .$$

Here $\widehat{\mathbf{F}}_m^k$ is the bilinear patch defined by:

$$\widehat{\mathbf{F}}_m^k(u,v) = (1-v)[(1-u)\overline{\mathbf{b}}_{0,0} + u\overline{\mathbf{b}}_{3,0}] + v[(1-u)\overline{\mathbf{b}}_{0,3} + u\overline{\mathbf{b}}_{3,3}] \ , \tag{9}$$

where $(u,v) \in \Omega$. Let $\Omega_m^k = [u_0, u_1] \times [v_0, v_1]$. Then,

$$\begin{aligned}
&\overline{\mathbf{b}}_{0,0} = \overline{\mathbf{F}}(u_0, v_0) \ , \quad \overline{\mathbf{b}}_{3,0} = \overline{\mathbf{F}}(u_1, v_0) \ , \\
&\overline{\mathbf{b}}_{0,3} = \overline{\mathbf{F}}(u_0, v_1) \ , \quad \overline{\mathbf{b}}_{3,3} = \overline{\mathbf{F}}(u_1, v_1) \ .
\end{aligned}$$

Similarly to the analysis in Section 3, we can rewrite $\mathbf{S}_m^k(u,v)$ and $\widehat{\mathbf{F}}_m^k(u,v)$ into the bicubic Bézier forms as Eqs. (4) and (6), respectively. Thus, for $(u,v) \in \Omega_m^k$, we have

$$\begin{aligned}
\|\mathbf{S}(u,v) - \overline{\mathbf{F}}(u,v)\| &= \|\mathbf{S}_m^k(\tilde{u},\tilde{v}) - \widehat{\mathbf{F}}_m^k(\tilde{u},\tilde{v})\| \\
&\leq \sum_{i=0}^{3}\sum_{j=0}^{3} \|\mathbf{b}_{i,j} - \overline{\mathbf{b}}_{i,j}\| B_i^3(\tilde{u}) B_j^3(\tilde{v}).
\end{aligned} \tag{10}$$

Notice that $\widehat{\mathbf{F}}_m^k$ is not the limit face of the B-spline patch $\mathbf{S}_m^k$ but one portion of the extraordinary patch $\mathbf{S}$'s limit face $\overline{\mathbf{F}}$. So we can not use the results for $\|\mathbf{b}_{i,j} - \overline{\mathbf{b}}_{i,j}\|$ derived in Section 3.

4.1 Distance bound

As k increases, the expression of $\mathbf{b}_{i,j} - \overline{\mathbf{b}}_{i,j}$ may be too complicated to decomposed directly into the linear combination of the second order differences of the control points as done in Section 3. Fortunately, $\mathbf{b}_{i,j}$ and $\overline{\mathbf{b}}_{i,j}, 0 \leq i, j \leq 3$ are the convex combinations of the initial control points $\mathbf{P}_i, i = 1, 2, \ldots, 2n+8$, and $\mathbf{b}_{i,j} - \overline{\mathbf{b}}_{i,j}$ can always be expressed as the linear combinations of $2n+10$ SODs $\alpha_l, l = 1, 2, \ldots 2n+10$ defined in Eq. (1): [1]

$$\mathbf{b}_{i,j} - \overline{\mathbf{b}}_{i,j} = \sum_{l=1}^{2n+10} x_l^{i,j} \alpha_l \ ,$$

where $x_l^{i,j}, l = 1, 2, \ldots, 2n+10$ are undetermined real coefficients. It follows that:

$$\|\mathbf{b}_{i,j} - \overline{\mathbf{b}}_{i,j}\| \leq \sum_{l=1}^{2n+10} \|x_l^{i,j} \alpha_l\| \leq \sum_{l=1}^{2n+10} |x_l^{i,j}| \|\alpha_l\| \leq \sum_{l=1}^{2n+10} |x_l^{i,j}| M \ .$$

Therefore, to get a tight upper bound for $\|\mathbf{b}_{i,j} - \overline{\mathbf{b}}_{i,j}\|$, we solve the following constrained minimization problem:

$$\begin{aligned} c_{i,j} &= \min \sum_{l=1}^{2n+10} |x_l^{i,j}| \\ s.t. \quad & \sum_{l=1}^{2n+10} x_l^{i,j} \alpha_l = \mathbf{b}_{i,j} - \overline{\mathbf{b}}_{i,j} \ . \end{aligned} \tag{11}$$

SODs $\alpha_l, l = 1, 2, \ldots 2n+10$ and $\mathbf{b}_{i,j} - \overline{\mathbf{b}}_{i,j}$ can be expressed as the linear combinations of the initial control points $\mathbf{P}_i, i = 1, 2, \ldots, 2n+8$. Consequently, the constraint in Eq. (11) can be written into

$$X^{i,j} D\mathbf{P} = E^{i,j}\mathbf{P},$$

where $X^{i,j} = [x_1^{i,j}, x_2^{i,j}, \ldots, x_{2n+10}^{i,j}]$, $\mathbf{P} = [\mathbf{P}_1, \mathbf{P}_2, \ldots, \mathbf{P}_{2n+8}]^t$, D is a $(2n+10) \times (2n+8)$ matrix, and $E^{i,j}$ is a $1 \times (2n+8)$ row vector. Then, the constraint reduces to a linear constraint of the form:

$$X^{i,j} D = E^{i,j} \ .$$

By solving 16 constrained minimization problems with the form as Eq. (11), we have:

$$\|\mathbf{b}_{i,j} - \overline{\mathbf{b}}_{i,j}\| \leq c_{i,j} M, \ 0 \leq i, j \leq 3 \ .$$

[1] For $3 \leq n \leq 50$, the statement has been verified using the symbolic computation of *Mathematica*. But we can't give a strict proof for a general $n, n \geq 3$, and then we leave it as an open problem.

Consequently, it follows from Eq. (10) that

$$\|\mathbf{S}_m^k(u,v) - \widehat{\mathbf{F}}_m^k(u,v)\| \leq \mathcal{B}_m^k(u,v)M,\ (u,v) \in \Omega\ ,$$

where the bicubic Bézier function

$$\mathcal{B}_m^k(u,v) = \sum_{i=0}^{3}\sum_{j=0}^{3} c_{i,j} B_i^3(u) B_j^3(v),\ (u,v) \in \Omega \tag{12}$$

is the *distance bound function* of $\mathbf{S}_m^k(u,v)$ with respect to $\widehat{\mathbf{F}}_m^k(u,v)$. And the *distance bound function* of $\mathbf{S}(u,v)$ with respect to $\overline{\mathbf{F}}(u,v)$, $\mathcal{B}(u,v), (u,v) \in \Omega$, can be defined as follows:

$$\mathcal{B}(u,v) \mid_{\Omega_m^k} = \mathcal{B}_m^k(\mathbf{t}_m^k(u,v)),\ k \geq 1, m = 1,2,3\ .$$

It is obvious that $\mathcal{B}(0,0) = \mathcal{B}(1,0) = \mathcal{B}(0,1) = \mathcal{B}(1,1) = 0$. Let $\beta_m^k(n) = \max_{(u,v)\in\Omega} \mathcal{B}_m^k(u,v)$, $k \geq 1, m = 1,2,3$, and $\beta(n) = \max_{k\geq 1, m=1,2,3} \beta_m^k(n)$, we have the following theorem on the maximal distance between $\mathbf{S}(u,v)$ and $\overline{\mathbf{F}}(u,v)$:

Theorem 6 *The distance between an extraordinary CCSS patch* $\mathbf{S}$ *and the corresponding limit face* $\overline{\mathbf{F}}$ *is bounded by*

$$\max_{(u,v)\in\Omega} \|\mathbf{S}(u,v) - \overline{\mathbf{F}}(u,v)\| \leq \beta(n)M\ , \tag{13}$$

where $\beta(n)$ *is a constant that depends only on* n*, the valence of* $\mathbf{S}$*'s extraordinary vertex, and* M *is the second order norm of* $\mathbf{S}$*'s initial control mesh.*

For $3 \leq n \leq 50$, by plotting the graph of $\mathcal{B}(u,v)$ and numerically computing $\beta_m^k(n)$ and $\beta(n)$, we obtain the following facts:

(1) If $n = 3$, $\beta(n) = \beta_2^2(n)$, i.e. $\mathcal{B}(u,v)$ attains its maximum in the tile Ω_2^2.
(2) If $n \geq 4$, $\beta(n) = \beta_2^1(n)$, i.e. $\mathcal{B}(u,v)$ attains its maximum in the tile Ω_2^1.

Therefore, we have the following algorithm to determine the constants $\beta(n), n \geq 4$:

Step 1. Compute the control points $\mathbf{p}_{i,j}, 0 \leq i,j \leq 3$ of $\mathbf{S}_2^1$ as described in Section 2.2, then determine the Bézier points $\mathbf{b}_{i,j}, 0 \leq i,j \leq 3$ of $\mathbf{S}_2^1$ according to Eq. (5).

Step 2. Calculate the limit points of $\mathbf{P}_1, \mathbf{P}_4, \mathbf{P}_5, \mathbf{P}_6$, and determine the expression of $\widehat{\mathbf{F}}_2^1$ according to Eqs. (8) and (9). Then compute the Bézier points $\overline{\mathbf{b}}_{i,j}, 0 \leq i,j \leq 3$ of $\widehat{\mathbf{F}}_2^1$ as explained in Section 3.1.

Step 3. Solve 10 constrained minimization problems with the form as Eq. (11) to get the bound constants $c_{i,j}, 0 \leq i \leq j \leq 3$. The remaining 6 constants

$c_{i,j}, 0 \leq j < i \leq 3$ can be determined by symmetry. Then, the distance bound function $\mathcal{B}_2^1(u,v), (u,v) \in \Omega$ can be obtained from Eq. (12).

Step 4. Finally, $\beta(n)$ is determined as the maximum of $\mathcal{B}_2^1(u,v), (u,v) \in \Omega$.

The algorithm has been implemented in *Mathematica* 5.1, and the involved optimization problems are solved using the numerical optimization package of *Mathematica* 5.1. Note that during the computation process of the first three steps, control points $\mathbf{P}_i, i = 1, 2, \ldots, 2n+8$ act as symbols and can be cancelled in the constraints of Step 3. These c_{ij} are independent of the initial control points because the constraint in Eq. (11) can reduce to a linear constraint independent of the initial control points. Consequently, $\beta(n)$ is a constant that depends only on the valence of $\mathbf{S}$'s extraordinary vertex.

$\beta(3) = 0.258146$ can be determined with a similar procedure. The values of $\beta(n), 3 \leq n \leq 50$ are plotted in Fig. 6. For $n > 4$, $\beta(n) < \beta(4) = \frac{1}{4}$. And for $3 \leq n \leq 48$, $\beta(n)$ strictly decreases as n increases.

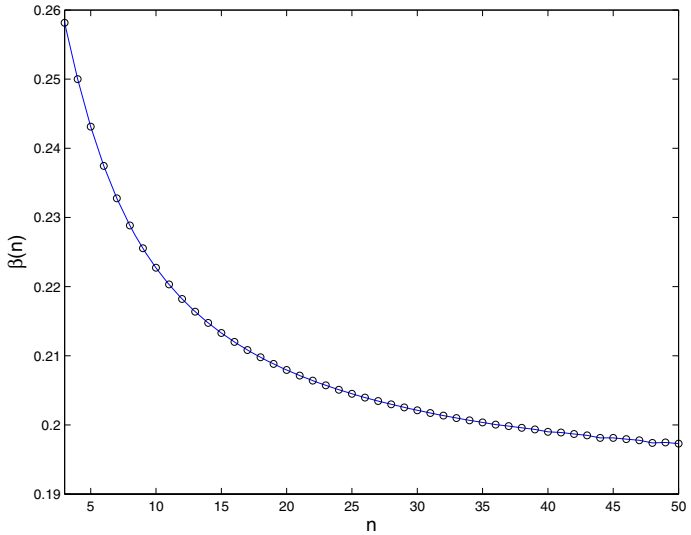

Fig. 6. Graph of $\beta(n)$, $3 \leq n \leq 50$.

5 Subdivision depth estimation

Given an error tolerance $\epsilon > 0$, the *subdivision depth* of a CCSS patch $\mathbf{S}$ with respect to ϵ is a positive integer d such that if the control mesh of $\mathbf{S}$ is recursively subdivided d times, the distance between the resulting limit mesh and $\mathbf{S}$ is smaller than ϵ.

The distance between an extraordinary CCSS patch $\mathbf{S}(u,v)$ and its level-1

limit mesh can be expressed as

$$\max_{i=0,1,2,3} \max_{(u,v)\in\Omega} \|\mathbf{S}_i^1(u,v) - \overline{\mathbf{F}}_i^1(u,v)\| \ ,$$

where $\mathbf{S}_i^1, i = 0,1,2,3$ are the level-1 subpatches of $\mathbf{S}$ as described in Section 2.2, and $\overline{\mathbf{F}}_i^1$ are the limit faces corresponding to $\mathbf{S}_i^1, i = 0,1,2,3$, respectively. It is easy to see that:

$$\max_{(u,v)\in\Omega} \|\mathbf{S}_0^1(u,v) - \overline{\mathbf{F}}_0^1(u,v)\| \le \beta(n) M_0^1 \le \beta(n) r_1(n) M^0 \ ,$$
$$\max_{(u,v)\in\Omega} \|\mathbf{S}_i^1(u,v) - \overline{\mathbf{F}}_i^1(u,v)\| \le \beta(4) M_i^1 \le \frac{1}{4} r_1(n) M^0, \ i = 1,2,3 \ .$$

It follows that:

$$\max_{i=0,1,2,3} \max_{(u,v)\in\Omega} \|\mathbf{S}_i^1(u,v) - \overline{\mathbf{F}}_i^1(u,v)\| \le \max\{\beta(n), \frac{1}{4}\} r_1(n) M^0 \ .$$

Because of the properties of $r_j(n), j \ge 0$, the distance between an extraordinary CCSS patch $\mathbf{S}(u,v)$ and its level-k limit mesh is bounded by:

$$\max_{i=0,1,\ldots,4^k-1} \max_{(u,v)\in\Omega} \|\mathbf{S}_i^k(u,v) - \overline{\mathbf{F}}_i^k(u,v)\| \le \max\{\beta(n), \frac{1}{4}\} r_k(n) M^0 \ .$$

Similarly to the derivation in (Huang and Wang, 2007), we have the following subdivision depth estimation theorem for CCSS patches.

Theorem 7 *Given a CCSS patch* $\mathbf{S}$ *of valence* n *and an error tolerance* $\epsilon > 0$*, after*

$$k = \min_{0\le j\le a-1} a l_j + j \tag{14}$$

steps of subdivision on $\mathbf{S}$*'s initial control mesh, the distance between* $\mathbf{S}$ *and its level-*k *limit mesh is smaller than* ϵ*. Here,*

$$l_j = \left\lceil \log_{\frac{1}{r_a(n)}} \left(\frac{r_j(n) \max\{\beta(n), \frac{1}{4}\} M}{\epsilon} \right) \right\rceil, \quad 0 \le j \le a-1, a \ge 1 \ .$$

In particular, for regular CCSS patches, $k = \left\lceil \log_4 \left(\frac{M}{4\epsilon}\right) \right\rceil$. For an extraordinary CCSS patch with $n > 4$, since $\beta(n) < \frac{1}{4}$, l_j can be simplified to $\left\lceil \log_{\frac{1}{r_a(n)}} \left(\frac{r_j(n) M}{4\epsilon}\right) \right\rceil$.

6 Comparison

Both a control mesh and its corresponding limit mesh can be employed to approximate a CCSS in practical applications. This section compares these two approximation representations.

The distance between a CCSS patch $\mathbf{S}$ of valence n and its control mesh is bounded as (Cheng et al., 2006; Chen and Cheng, 2006; Huang and Wang, 2007):

$$\max_{(u,v)\in\Omega} \|\mathbf{S}(u,v) - \mathbf{F}(u,v)\| \leq C_a(n)M \ . \tag{15}$$

And $C_a(n)$ can be unified as (Huang and Wang, 2007)

$$C_a(n) = \frac{1}{\min\{n,8\}} \frac{\sum_{j=0}^{a-1} r_j(n)}{1 - r_a(n)}, \ a \geq 1 \ .$$

The case where $a = 1$ corresponds to the result proposed in (Cheng et al., 2006), and the case where $a = 2$ is exactly as per the result presented in (Chen and Cheng, 2006). The distance estimates in Eqs. (13) and (15) are both expressed in terms of M, the second order norm of $\mathbf{S}$, and constants that depend on n which is the valence of $\mathbf{S}$.

Table 1
Comparison of $C_a(n), a = 1, 2$ and $\beta(n)$, $3 \leq n \leq 10$

n	$C_1(n)$	$C_2(n)$	$C_2(n)$	$\beta(n)$
3	1.000000	0.784314	0.784314	0.258146
4	0.333333	0.333333	0.333333	0.250000
5	0.714286	0.574890	0.574890	0.243129
6	0.705882	0.642267	0.549020	0.237454
7	0.717949	0.527357	0.527357	0.232761
8	0.695652	0.582436	0.424242	0.228848
9	0.736364	0.510181	0.510181	0.225549
10	0.757576	0.678442	0.519591	0.222738

Table 1 illustrates the comparison results of the constants $C_1(n)$, $C_2(n)$, and $\beta(n)$ for $3 \leq n \leq 10$. The values of $C_1(n)$ in the second column are evaluated with the approach derived by Cheng et al. (2006). The values of $C_2(n)$ in the third and fourth columns are computed with the techniques proposed by Chen and Cheng (2006) and Huang and Wang (2007), respectively. It can be seen that $C_a(4) = \frac{1}{3}$ is the smallest of $C_a(n), n \geq 3$ but $\beta(4) = \frac{1}{4}$ is the biggest of

$\beta(n), n \geq 4$. $\beta(n) < C_a(n), n \geq 3$ shows that the limit mesh approximates a CCSS better than the corresponding control mesh in general.

Given a CCSS patch $\mathbf{S}$ of valence n and an error tolerance $\epsilon > 0$, the subdivision depth estimation formula for the control mesh approximation is expressed as follows (Huang and Wang, 2007):

$$k = \min_{0 \leq j \leq a-1} a\ l_j + j\ \ , \tag{16}$$

where

$$l_j = \left\lceil \log_{\frac{1}{r_a(n)}} \left(\frac{r_j(n) C_a(n) M}{\epsilon} \right) \right\rceil, \quad 0 \leq j \leq a-1,\ a \geq 1\ \ .$$

The cases where $a = 1$ and $a = 2$ correspond to the formulas derived in (Cheng et al., 2006) and (Chen and Cheng, 2006), respectively. For regular patches, $k = \left\lceil \log_4 \left(\frac{M}{3\epsilon} \right) \right\rceil$.

Although $\beta(n)$ is much smaller than $C_a(n)$, the convergence rates of the second order norm, $r_j(n), 0 \leq j \leq a$, play the major role in subdivision depth estimation. For example,

$$0 < \log_4 \left(\frac{M}{3\epsilon} \right) - \log_4 \left(\frac{M}{4\epsilon} \right) = \log_4 \frac{4}{3} < 1$$

means that for regular CCSS patches, to satisfy the same error tolerance control mesh approximation needs at most one more subdivision step than limit mesh approximation. Notice that at each subdivision step, the number of quadrilaterals quadruples. One less step implies that the number of faces in the limit mesh approximation is a quarter of the number in the control mesh approximation.

Table 2
Comparison of subdivision depths

n	3	4	5	6	7	8	9	10
Cheng et al. (2006)	14	4	16	19	23	26	27	28
Chen and Cheng (2006)	9	4	11	16	14	18	16	22
Huang and Wang (2007)	9	4	11	13	14	13	16	17
limit mesh approx.	6	3	8	10	11	11	12	12

Table 2 shows the comparison results for subdivision depths for the two representations. The error tolerance ϵ is set to 0.01, and the second order norm M is assumed to be 2. The first three rows are the results for control mesh approximation, computed with the direct decomposition method (Cheng et al.,

2006), the matrix based technique (Chen and Cheng, 2006), and the optimization based approach (Huang and Wang, 2007), respectively. The last row is the depths in the limit mesh approximation. As can be seen from the table, the limit mesh approximation shows a 30%–50% improvement over control mesh approximation in most of the cases.

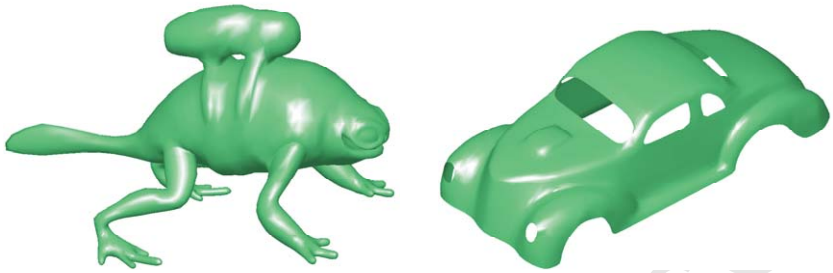

Fig. 7. Limit surfaces of a frog model (*left*) and a car model (*right*)

In the following, we compare the number of mesh faces needed to satisfy the same precision, in a control and a limit mesh approximation to a CCSS. Given an error tolerance ϵ, we can first estimate the subdivision depth for each patch according to Eqs. (14) and (16), then uniformly subdivide each patch correspondingly. However, even applying uniform subdivision to one extraordinary patch, a large number of faces are required to produce a high accurate approximation (Huang and Wang, 2007). Therefore, we apply the error controlled adaptive subdivision, proposed by Huang and Wang (2007), to a closed surface - a frog model (see Fig. 7 *left*) and an open surface - a car model (see Fig. 7 *right*).

Table 3
Comparison of the numbers of faces in control and limit mesh approximations after adaptive subdivision

ϵ	Frog model		Car model	
	Control mesh	Limit mesh	Control mesh	Limit mesh
0.1	25,642	14,527	14,717	8,285
0.05	43,864	26,482	24,905	14,375
0.01	172,159	113,713	97,704	58,805

Table 3 illustrates the numbers of faces in control and limit mesh approximations for error tolerances 0.1, 0.05 and 0.01, respectively. Results show that the limit mesh approximations reduce the number of faces by about 30%, compared to the control mesh approximations. Thus, limit mesh approximation can improve performance in high accuracy CCSS rendering.

7 Conclusion

In this paper the approximation of a Catmull-Clark subdivision surface by its limit mesh is investigated. By introducing a distance bound function, we propose a bound on the distance between a CCSS patch and its limit face in terms of the second order norm of the control points and a constant that depends on the valence of the patch. A subdivision depth estimation formula for a CCSS patch is also derived.

In general, a limit mesh approximates the limit surface better than the corresponding control mesh. This means that, compared with control mesh approximation, limit mesh approximation has a smaller subdivision depth and, consequently, requires fewer faces for a given error tolerance. The test results show that limit mesh approximation improves on control mesh approximation by about 30% in most of the cases. Thus, for a CCSS, a limit mesh is more appropriate in rendering and other applications.

Our analysis techniques can be easily extended to other spline based subdivision surfaces, such as Doo-Sabin subdivision surfaces (Doo and Sabin, 1978) and Loop subdivision surfaces (Loop, 1987). We will explore these in a forthcoming paper.

Acknowledgements

We would like to thank the anonymous reviewers for their valuable comments. This work was supported by the 973 Program of China (No. 2004CB719403), the 863 Program of China (Nos. 2006AA01Z334 and 2007AA01Z318), NSF of China (Nos. 10671192, 60573151 and 60473100), and the China Postdoctoral Science Foundation (No. 20060390359).

References

Catmull, E., Clark, J., 1978. Recursively generated B-spline surfaces on arbitrary topological meshes. Computer-Aided Design 10 (6), 350–355.

Chen, G., Cheng, F., 2006. Matrix based subdivision depth computation for extra-ordinary Catmull-Clark subdivision surface patches. In: Proceedings of GMP 2006 (LNCS 4077). Springer, Berlin Heidelberg, pp. 545–552.

Cheng, F., Chen, G., Yong, J., 2006. Subdivision depth computation for extra-ordinary Catmull-Clark subdivision surface patches. In: Proceedings of CGI 2006 (LNCS 4035). Springer, Berlin Heidelberg, pp. 404–416.

Cheng, F., Yong, J., 2006. Subdivision depth computation for Catmull-Clark subdivision surfaces. Computer Aided Design & Applications 3 (1–4), 485–494.

Doo, D., Sabin, M. A., 1978. Behaviour of recursive subdivision surfaces near extraordinary points. Computer-Aided Design 10 (6), 356–360.

Farin, G., 2002. Curves and Surfaces for Computer-Aided Geometric Design — A Practical Guide, 5th Edition. Morgan Kaufmann Publishers, San Francisco.

Halstead, M., Kass, M., DeRose, T., 1993. Efficient, fair interpolation using Catmull-Clark surfaces. In: Proceedings of SIGGRAPH 93. ACM, New York, pp. 35–44.

Hoppe, H., DeRose, T., Duchamp, T., Halstead, M., Jin, H., McDonald, J., Schweitzer, J., Stuetzle, W., 1994. Piecewise smooth surface reconstruction. In: Proceedings of SIGGRAPH 94. ACM, New York, pp. 295–302.

Huang, Z., Wang, G., 2007. Improved error estimate for extraordinary Catmull-Clark subdivision surface patches. The Visual Computer 23 (12), 1005–1014.

Loop, C. T., August 1987. Smooth subdivision surfaces based on triangles. Master's thesis, Department of Mathematics, University of Utah.

Lutterkort, D., Peters, J., 2001. Tight linear envelopes for splines. Numerische Mathematik 89 (4), 735–748.

Mustafa, G., Chen, F., Deng, J., 2006. Estimating error bounds for binary subdivision curves/surfaces. Journal of Computational and Applied Mathematics 193 (2), 596–613.

Mustafa, G., Deng, J., 2007. Estimating error bounds for ternary subdivision curves/surfaces. Journal of Computational Mathematics 25 (4), 473–484.

Nairn, D., Peters, J., Lutterkort, D., 1999. Sharp, quantitative bounds on the distance between a polynomial piece and its Bézier control polygon. Computer Aided Geometric Design 16 (7), 613–631.

Reif, U., 2000. Best bounds on the approximation of polynomials and splines by their control structure. Computer Aided Geometric Design 17 (6), 579–589.

Stam, J., 1998. Exact evaluation of Catmull-Clark subdivision surfaces at arbitrary parameter values. In: Proceedings of SIGGRAPH 98. Annual Conference Series. ACM, New York, pp. 395–404.

Wang, H., Qin, K., 2004. Estimating subdivision depth of Catmull-Clark surfaces. Journal of Computer Science and Technology 19 (5), 657–664.